






## The flexural and compressive properties of sandwich composites with different 3D-printed core structures

 Rabia Caran<sup>a,b</sup>,  Ayten Nur Yüksel Yılmaz<sup>a,c</sup>,  Necati Ercan<sup>c</sup>,  Doruk Erdem Yunus<sup>c</sup>  
and  Ayşe Çelik Bedeloğlu<sup>a,\*</sup>

<sup>a</sup>Department of Polymer Materials Engineering, Bursa Technical University, Bursa, Turkey.

<sup>b</sup>Structural Manufacturing R&D Department, BAYKAR Technology, İstanbul, Turkey.

<sup>c</sup>Department of Mechanical Engineering, Bursa Technical University, Bursa, Turkey.

### ARTICLE INFO

#### Article history:

Received 5 September 2023

Received in revised form 19 October 2023

Accepted 18 November 2023

Available online

#### Keywords:

3D-Printed core

Fused deposition modeling (FDM)

Sandwich composite

Carbon fiber-reinforced polyactic acid

Compressive properties

Flexural properties

### ABSTRACT

In this study, different core structures are produced with polylactic acid (PLA) and carbon fiber reinforced PLA (CFR-PLA) filaments using a 3D printer with fused deposition modeling (FDM) technique. An alternative new core structure is proposed to the honeycomb and square core structures commonly used in the literature. Then, sandwich composites are produced by bonding carbon fiber-epoxy plates to the lower and upper surfaces of these core structures. The effect of carbon fiber reinforcement and core types on the mechanical properties of sandwich composites was investigated. The core structures produced with carbon fiber-reinforced PLA showed lower compressive strength but higher compressive modulus than those produced with pure PLA. Among the core structures, the designed structure showed the highest compressive strength with a value of 9.867 MPa, which is 32.18% and 54.36% higher than the honeycomb and square structure. While the flexural strength and flexural stiffness of the sandwich composites increased with carbon fiber reinforcement, the designed sandwich composite showed approximately 1.40 and 3.15 times the flexural strength of the honeycomb and square sandwich composites, respectively.

## I. INTRODUCTION

Unmanned aerial vehicles (UAVs) are aircraft that fly autonomously with an autopilot without human assistance [1]. UAVs have significant advantages such as minimal operating cost, reduced human error, and the ability to operate under hazardous conditions [2]. UAVs were first introduced during the Second World War and have progressed significantly over time [3]. In recent years, research and development studies of UAVs have attracted great attention not only for the military but also for civilian applications [4]. UAVs are preferred in many applications such as meteorological data collection, disaster monitoring, search and rescue activities, telecommunications, mapping, surveillance, payload deliveries (disposable load), reconnaissance, and attack [5–10].

The primary feature desired from materials used in the aerospace industry is that they have low-weight and high strength. This is expressed by the term specific strength and is defined as the strength of the unit weight of the material. UAV components with high specific strength provide solutions to many situations such as longer flight distances, reducing emissions, and responding to safety requirements [11]. Successful development of UAVs depends on the production of low-cost and high-resilience platforms. Reducing the structural weight is one of the effective factors to improve the performance of UAVs and increase their disposable load (payload) capacity [10].

\*Corresponding author. Tel.: +90-224-300-3491; e-mail: ayse.bedeloglu@btu.edu.tr

For this purpose, aviation designers aim to reduce the weight of the UAV. This encourages the researchers to develop stronger materials and better structural designs.

Composite materials are formed as a result of combining two or more materials to obtain materials having new (desired) properties. These materials have many advantages such as high strength, low weight, high corrosion and chemical resistance, and high fatigue strength [12]. Therefore, composite materials have gradually replaced metals in the aerospace and UAV industries and are already frequently used [13, 14]. Using only strong materials is not sufficient to reduce the weight of the UAV. In this case, it is necessary to offer design improvements. Lattice structures are a good alternative to increase the specific strength of UAV components. Lattice structures are often geometrically complex and difficult to manufacture using traditional manufacturing techniques such as molding or milling [15]. Since lightweight structures with complex geometries are difficult and costly to produce using traditional fabrication methods, lattice structures can be directly printed by Additive Manufacturing (AM).

AM helps to improve the aerodynamic and structural efficiency of UAVs with the design freedom feature it offers to users [3, 10]. AM is an innovative manufacturing technique where the final product is produced layer by layer using the CAD file directly [16, 17]. AM has many application areas such as aerospace, automotive, biomedical so on [18, 19]. Metals, polymers, ceramics, and composites are preferred as materials in Additive Manufacturing (AM) in aerospace applications [20–23]. Additive manufacturing methods such as Fused Deposition Modeling (FDM), Selective Laser Sintering (SLS), Stereolithography (SLA), Selective Laser Melting (SLM), and Electron Beam Melting (EBM) are used to produce UAV components [3]. FDM is the most widely used additive manufacturing method with some advantages [10, 24, 25]. FDM is based on the principle of melting a thermoplastic polymer filament in a printhead and extruding the molten material on a print bed. Many studies have been conducted in which critical parts of UAVs are manufactured using the FDM method. For example, Stratasys and Aurora Flight Sciences have produced the largest and fastest AM drone (UAV) using FDM [26]. Paskalya et al. have printed UAV wings from acrylonitrile-butadiene-styrene (ABS) material with FDM [27]. In another study, an optimized UAV landing gear was designed and manufactured using the FDM method [2]. There are many studies that use the FDM method to print UAV parts [3, 10, 28–30].

The most widely used thermoplastic filaments to manufacture UAV components with FDM are Acrylonitrile Butadiene Styrene (ABS), Polylactic Acid (PLA), Polyetherimide (ULTEM), Polyphenylene Sulfide (PPS), Polycarbonate (PC), Polyamide (Nylon), Polyethylene Terephthalate Glycol (PETG), etc. [31, 32]. These thermoplastic materials have relatively low strength and are often used in applications where strength is not very necessary. However, thermoplastic filaments are not suitable for applications where high stresses occur, such as landing gear. To increase the strength of the parts to be used in aerospace applications, it is necessary to strengthen the thermoplastic filaments with reinforcements [33]. FDM is one of the AM methods by which reinforced thermoplastics can be printed [34]. Thermoplastics used in FDM are reinforced with materials such as metal, graphene and carbon to increase the strength [29, 35, 36]. The most commonly used reinforcement is Carbon Fiber (CF), and Thermoplastic/CF filaments are often preferred in aviation and UAV applications [37–41].

Adding carbon fibers to thermoplastic filaments is generally made in two different ways as discontinuous (short) and continuous fiber. Research has generally focused on discontinuous fiber-reinforced composites because additive manufacturing of continuous fiber-reinforced composites involves some difficulties and is costly [42–44]. Short fiber-reinforced (discontinuous) FDM composites are formed by blending the thermoplastic polymer with

milled or chopped fibers. Then, the blending is extruded to form filaments, which are the raw materials of the FDM method. Fibers are typically shorter than the nozzle diameter to avoid clogging [45, 46]. The majority of fibers used in AM composites are milled fibers and have a fiber length of fewer than 150  $\mu\text{m}$  [47].

While short fiber-reinforced polymer composites produced by AM offer significant performance improvements compared to pure polymers (PLA, ABS, PETG), the maximum mechanical properties achieved with short fiber-reinforced composites are severely limited compared to continuous fiber polymer composites [30]. There are several reasons why the mechanical properties obtained by additive manufacturing of short fiber reinforced filaments are unsatisfactory. The first reason is that milled fibers are not effective enough to increase strength, as the fiber length of milled fibers is well below the value that provides optimum mechanical properties. In addition, it is known that the addition of fiber fillers will change the polymer rheology and therefore increase the void fraction in composites produced by AM [46]. Finally, mechanical properties are negatively affected when the interfacial bonds between the fiber and the thermoplastic matrix are not strong enough. As a result, the strength of 3D printed specimens is adversely affected due to defects such as high void content, poor interlayer bonding, and inhomogeneous fiber distribution [48–52]. For all these reasons, it has been observed that the specimens produced with CF-reinforced filament generally do not marginally increase the strength of those produced with pure polymer, and in some cases reduce it [47, 51, 53].

Sandwich materials, which are among the most valuable structural engineering materials of the composite material industry, are frequently used in aerospace and other industry fields for the advantages they offer such as low weight, high strength, and low production costs [54]. Typically sandwich structures consist of high-strength face sheets on the outer surfaces and the core with low weight in the middle. The core is mostly subjected to shear stresses while the face sheets on the surface are subjected to tensile and compression stresses [55]. The use of lightweight sandwich structures in UAVs provides better acceleration and lower fuel consumption by reducing the structural weight [56]. The most common traditional materials used in the core of lightweight sandwich structures are foam and balsa [57, 58]. Recently, researchers prefer functionally adjustable lattice structures as core materials in sandwich composites instead of traditional core materials after the recent developments in AM [59]. The desired functional properties in sandwich structures can be adjusted by changing the design or material of the cell structure. The studies show that various cellular structures such as honeycomb, gyroid, truss, diamond, kagome, octet, and hybrid are used as cores in sandwich composites [53, 60–64]. Therefore, the flexural and compressive properties of sandwich composites with different 3D-printed core structures developed for unmanned aerial vehicles were investigated in this study. Three different lattice structures were used as the core of the sandwich composite to achieve this goal: honeycomb, square, and original design. Sandwich composite specimens were created by affixing CF face sheets to a lattice-structured core made of PLA and CFR-PLA materials. The mechanical properties of sandwich structures were investigated in terms of cell topology and reinforced filaments.

## II. EXPERIMENTAL METHOD / TEORETICAL METHOD

### 2.1 Materials

In this study, two different filaments, polylactic acid (PLA) and 15% carbon fiber reinforced- PLA (CFR-PLA), were used. PLA filaments were purchased from Filament Dünyası (Turkey) and Sunlu brand CFR-PLA filament

was used. The diameter of the filaments is 1.75 mm. For each test, it was produced with both PLA and CFR-PLA in three designs. In the production of sandwich composites, plain woven carbon fabric with a density of 245 gr/m<sup>2</sup> was used as a reinforcement element on the lower and upper surfaces of the core structures. These carbon fabrics were provided by BAYKAR Technology (Turkey). EPORES 11564 epoxy and EPOHARD 13486 hardener were purchased from Omnis Kompozit (Turkey).

## 2.2 Design of core structures

In this study, 3 different core structures were produced by the FDM method using Creality Ender 3 Pro printer. In addition to the honeycomb and square structure used in the literature [9, 64, 65], a new design has been developed. The designed core structure has unit cells consist of 2 types of quadrilateral shapes which includes an inner rhombus supporting an outer rectangle (Figure 1). The short side, long side, and wall thicknesses of a unit of the core structure were preferred as 10 mm, 20 mm, and 0.5 mm, respectively. The height of the cell was chosen as 15 mm. Honeycomb and square structures were drawn in the same dimensions by using SolidWorks so that the designed core structure could be compared with traditional honeycomb and square structures. The length of one unit honeycomb cell in the honeycomb structure and the edge length of one unit cell of the square structure are 10 mm.

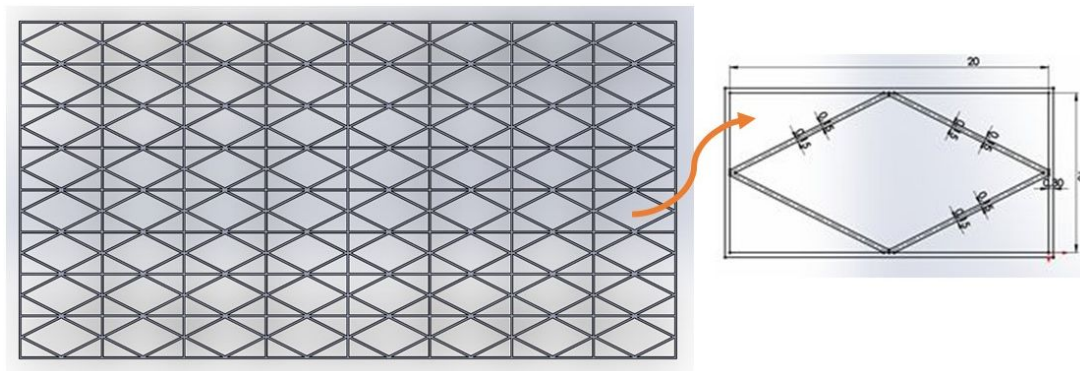


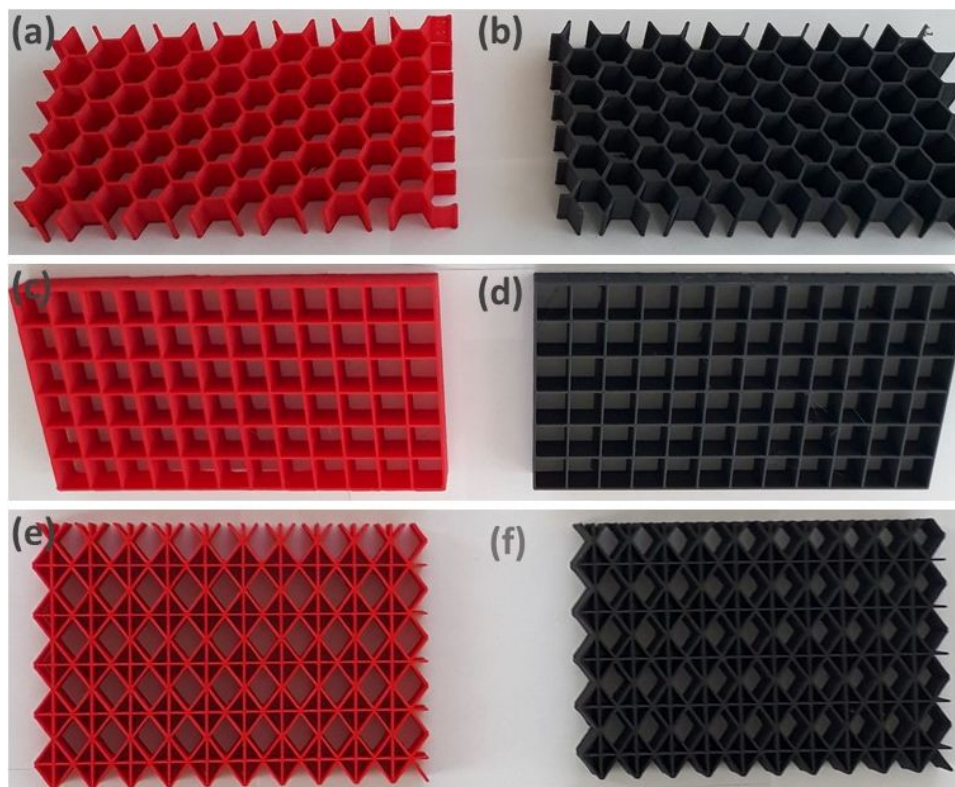
Figure 1. Image of the designed core structure

## 2.3 The manufacturing process of core structures

Honeycomb, square, and designed core structures were fabricated using a 3D printer (Creality Ender 3 Pro). These structures were produced with both PLA and CFR-PLA filaments. Processing parameters are given in Table 1. To begin, the geometry of the specimens was drawn in SolidWorks and exported as an STL file. The transferred geometry was opened in the Cura software and the appropriate parameters were entered and the specimens were printed on a 3D printer. Figure 2 shows the images of the core structures printed. The honeycomb, square, and newly designed core structure are denoted by the letters H, S, and D, respectively. In addition, the word CFR was added to these core structures produced with PLA filaments containing carbon fiber. For example, the abbreviation S-CFR-PLA refers to the square core structure produced with carbon fiber reinforced PLA filament, and H-PLA shows the honeycomb core structure produced with neat-PLA filament.

**Table 1.** The 3D printing process parameters

Printing Parameters	PLA	CFR-PLA
Extruder temperature (°C)	225	220
Bed temperature (°C)	80	80
Layer thickness (mm)	0.2	0.2
Infill density (%)	100	100
Flow rate (%)	105	95
Printing speed(mm/s)	50	50
Filament diameter (mm)	1.75	1.75

**Figure 2.** Images of (a) H-PLA, (b) H-CFR-PLA, (c) S-PLA, (d) S-CFR-PLA, (e) D-PLA, and (f) D-CFR-PLA specimens

#### 2.4 Manufacturing of sandwich composites

The sandwich composite specimens produced consist of three components: core structure, face sheets, and adhesive. For the production of the lower and upper face sheet layers, woven carbon fabric was used as a reinforcement, and epoxy resin was used as a matrix material. The production steps of sandwich composite specimens are shown in Figure 3. For the specimens to be easily separated from the surface, vacuum nylon was laid on the floor and 4 layers of carbon fiber were placed on top of each other (Figure 3a). On each layer, carbon fiber was wetted with an epoxy-hardener mixture (100:34 by weight) with the help of a brush. Then, a core structure was placed on top of the carbon fiber and 4 layers of carbon fiber were laid on top of this core structure (Figure 3b). Afterward, the specimens were covered with vacuum nylon and a heavy plate was placed on top and left to cure for 2 days. Figure 3c shows the side view of the sandwich composite specimens obtained at the end of the production stages.



**Figure 3.** Production steps of sandwich composite specimens: (a) placement of carbon fabrics in the lower part of the core structure, (b) placement of carbon fabrics in the upper part of the core structure, and (c) sandwich composites produced.

## 2.5 Test Procedure

### 2.5.1 Compression test

A compression test was applied to each core structure specimen consisting of two different filament materials (PLA and CRF-PLA) and three different designs (honeycomb, square, and design). The tests were performed with Shimadzu brand AG-X-plus model mechanical device having a load capacity of 250 kN according to ASTM C365–03 standard [66]. Dimensions of compression test specimens are 77x77x15 mm (length, width, and height). All tests were performed at a crosshead speed of 1 mm/min. During the test, the compressive load was increased until the maximum load that the specimens could carry, then decreased, and a visible deformation was obtained on the specimen along the height where the cell walls were compressed, and the results were recorded. The compressive strength ( $\sigma_c$ ) and compressive modulus ( $E_c$ ) values of the core structures were calculated with the following equations using the load and deflection data obtained from the test:

$$\sigma_c = P/A \quad (1)$$

$$E_c = \frac{\Delta P * t}{\Delta h * A} \quad (2)$$

where P, A,  $\Delta P$ ,  $\Delta h$ , and t show compressive load (N), cross-sectional area (mm<sup>2</sup>), the is the load increment in the elastic part of the compressive curve (N), the deflection increment corresponding to  $\Delta P$  (mm), and core thickness (mm), respectively. At least 5 compressive test specimens were tested for each set and average values were used.

### 2.5.2 Flexural test

Three-point bending tests were carried out on the sandwich composites formed by adding a face sheet layer made of carbon fiber and epoxy to the lower and upper sides of the core structures. Tests were performed on sandwich composites with SHIMADZU - AGS-X (250kN) device according to ASTM C 393–00. Specimen dimensions

were 120×60×15 mm (length, width and height). The test speed and span length, which is the length between the two end supports, were 0.75 mm/min and 80 mm, respectively.

The flexural strength ( $\sigma_f$ ) values of the sandwich specimens were calculated with the following equations according to ASTM C 393–00:

$$\sigma_f = PL/2t(d + c)b \quad (3)$$

where P, L, t, d, c, and b indicate flexural load (N), span length (mm), facing thickness (mm), sandwich thickness (mm), core thickness (mm), and sandwich width (mm), respectively. Also, the bending stiffness values of specimens were calculated by dividing the maximum bending force by the bending deflection at that load.

### III. RESULTS AND DISCUSSIONS

Firstly, compression tests of 3 different core structures produced using PLA and CFR-PLA filaments were carried out. Then, bending tests of sandwich composites produced using these core structures were performed. The acquired results are presented and assessed in the following subsections.

#### 3.1 Compressive test results

The compression properties of core structures are affected by various factors such as filament type, shape, and dimensions of the unit cell, and FDM process parameters [67–69]. The compressive properties of specimens with different filaments (PLA and CFR-PLA) and core structures (honeycomb, square, and design) are obtained from compression tests and the specimens properties are compared to each other. During the test, the specimens were compressed by applying force, as can be seen in Figure 4a. Also, Figures 4b and 4c show images of the specimens after testing.

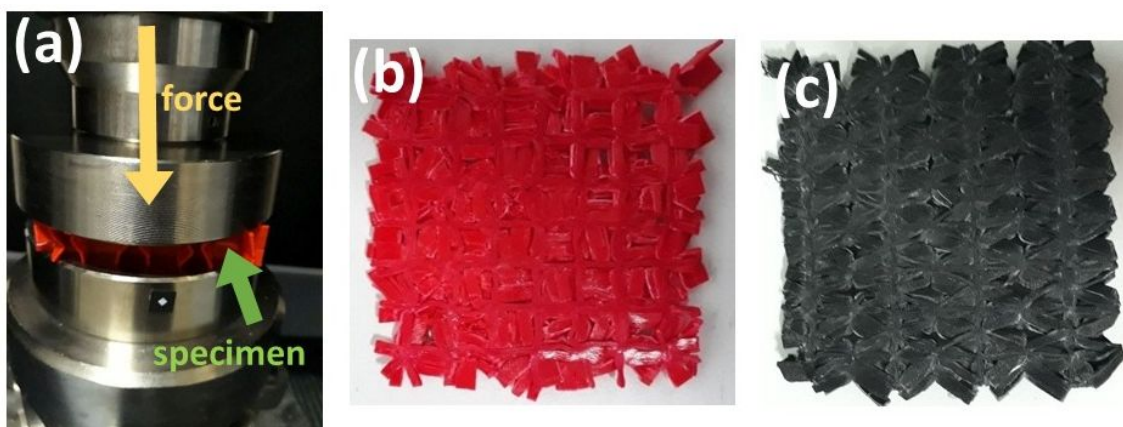


**Figure 4.** Image of a specimen in the compressive test (a), images of (b) S-PLA and (c) S-CFR-PLA specimens after the compressive test

Compressive test results of 3D printed specimens are summarized in Table 2. For each specimen set (H-PLA, H-CFR-PLA, S-PLA, S-CFR-PLA, D-PLA, D-CFR-PLA) at least five tests were conducted, the results were averaged, and the ultimate compressive strength, compressive strain at peak load, compressive modulus are listed. Compressive-strain curves of the three types of specimens are illustrated in Figure 5. When the stress-strain curves of the specimens are examined, it is seen that three different regions occur under compression loading. In the first region, a linear curve was observed until the maximum stress value was reached with the applied compressive force. The strain in this region is elastic. In other words, when the applied force is removed, the core structure returns to its original shape. The second region includes plastic yielding and ends by plateau stress. In this region, the stress value remains approximately constant for a long time, while the strain continues to increase. The constant stress value in this region is called plateau stress. The strain in the second region is plastic. If the structures continue to be compressed, the cell walls will be crushed and come into contact with each other, leading to a rapid increase in stress. This region is referred to as the densification region [70–73]. The core structures containing carbon fiber reinforced-PLA filament showed lower compressive strength than those containing pure PLA filament (Figures 6a and 6b). D-PLA showed the highest compressive strength value of 9.867 MPa. Compared to H-PLA and S-PLA, D-PLA compressive strength is approximately 32.18% and 54.36% higher, respectively. Saleh and his team printed diamond, gyroid, and primitive cell structures using both PLA and CF-reinforced PLA through the FDM method, investigating the impact of CF reinforcement on the mechanical properties of different core structure. The specimens produced with CF-PLA exhibited lower compressive strength compared to those produced with PLA. Among structures printed with both PLA and CF-PLA, the highest compressive strength was observed in specimens with a diamond cell structure, followed by Gyroid and Primitive cell structures. It was noted that Gyroid and Primitive cell structures deformed uniformly, allowing for consistent load-bearing. Additionally, it was mentioned that deformation became more uniform with an increase in relative density and a decrease in cell size [73]. This was attributed to the high surface area and improved material distribution, which enhanced the contact between walls and minimized the empty spaces between them.

**Table 2.** Compressive test results of core structures

Specimens	Ultimate compressive strength (MPa)	Compressive strain at peak load ( $\epsilon$ )	Compressive modulus (MPa)
H-PLA	7.465 $\pm$ 0.13	0.0581 $\pm$ 0.0058	167.088 $\pm$ 6.03
H-CFR-PLA	5.688 $\pm$ 0.26	0.0436 $\pm$ 0.0041	173.605 $\pm$ 5.30
S-PLA	6.392 $\pm$ 0.24	0.0429 $\pm$ 0.0052	164.803 $\pm$ 2.05
S-CFR-PLA	5.093 $\pm$ 0.17	0.0411 $\pm$ 0.0024	168.613 $\pm$ 4.58
D-PLA	9.867 $\pm$ 0.28	0.0611 $\pm$ 0.0066	169.728 $\pm$ 1.26
D-CFR-PLA	6.050 $\pm$ 0.13	0.0568 $\pm$ 0.0023	180.127 $\pm$ 4.51

However, core structures produced with CFR-PLA filament showed higher compressive modulus than those produced with pure PLA. The high elastic modulus of carbon fiber has increased the elastic modulus of core structures [72, 74]. In the study conducted by Mei et al., specimens printed with carbon fiber reinforced PLA showed higher compression modulus but lower compression strength than those printed with pure PLA. The following are the explanations given for the decrease in compressive strength of the specimens: Low compressive strength of the carbon fiber, agglomeration of the carbon fiber, and faults that may occur during the 3D printing



process [72]. In addition, buckling and layer separation may occur with the application of compressive force to the specimens produced by the FDM method, and this causes a decrease in the compressive strength [13, 75].

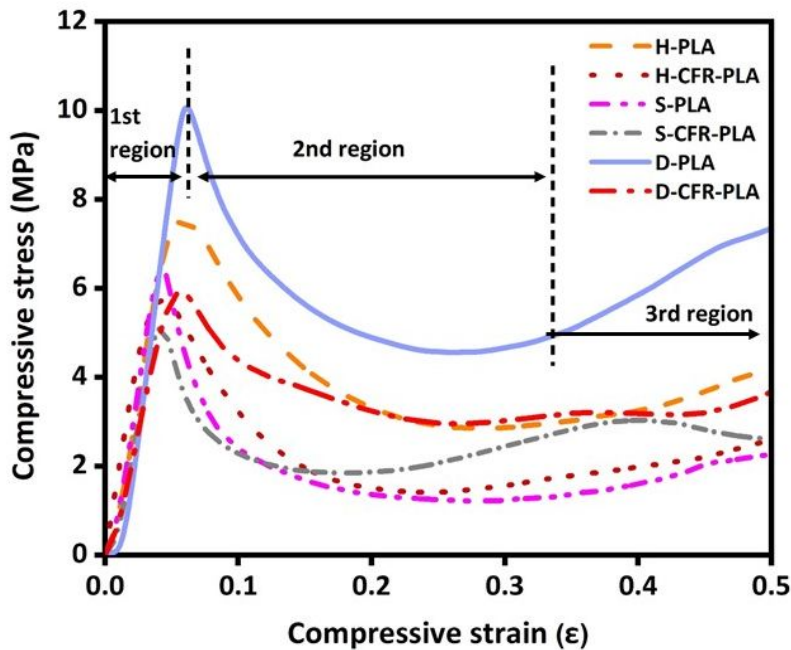


Figure 5. Compressive stress-strain curve of core specimens

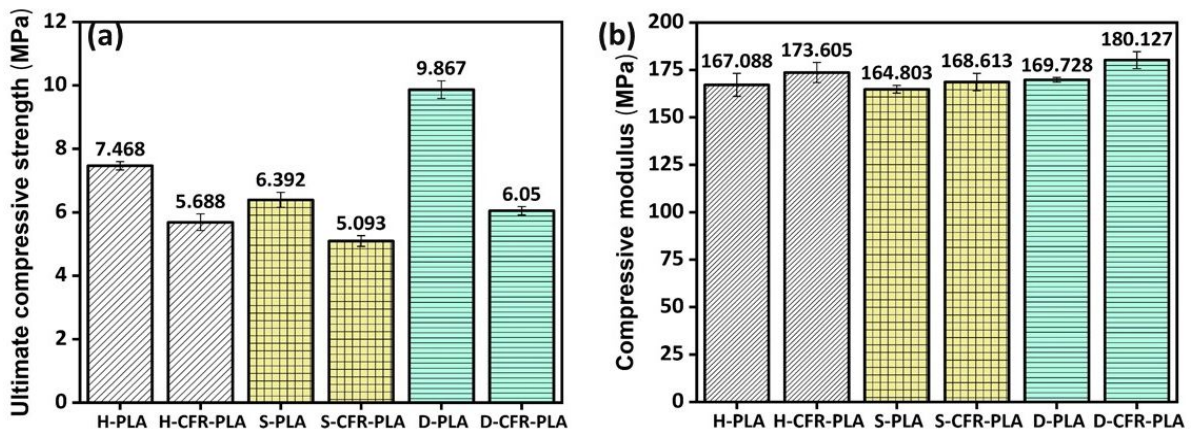


Figure 6. Ultimate compressive strength (a) and compressive modulus (b) of core structures

### 3.2 Flexural test results

Bending tests of sandwich composites, which were formed by bonding carbon fabric with epoxy to the lower and upper surfaces of different core structures produced by the FDM method, were carried out. Figure 7a shows a sandwich composite specimen subjected to bending force using a mechanical tester. After the bending test, cracks were observed in the core layer of all specimens in general (Figure 7b). These cracks occurred close to where the

bending force was applied (near the middle of the specimen). The bending test results of sandwich composites are summarized in Table 3. At least 5 tests were performed for each composite set (H-PLA, H-CFR-PLA, S-PLA, S-CFR-PLA, D-PLA, D-CFR-PLA) and the results were averaged. The force-deflection data of the composites were recorded during the test and facing bending stress and flexural stiffness values were calculated using these data.

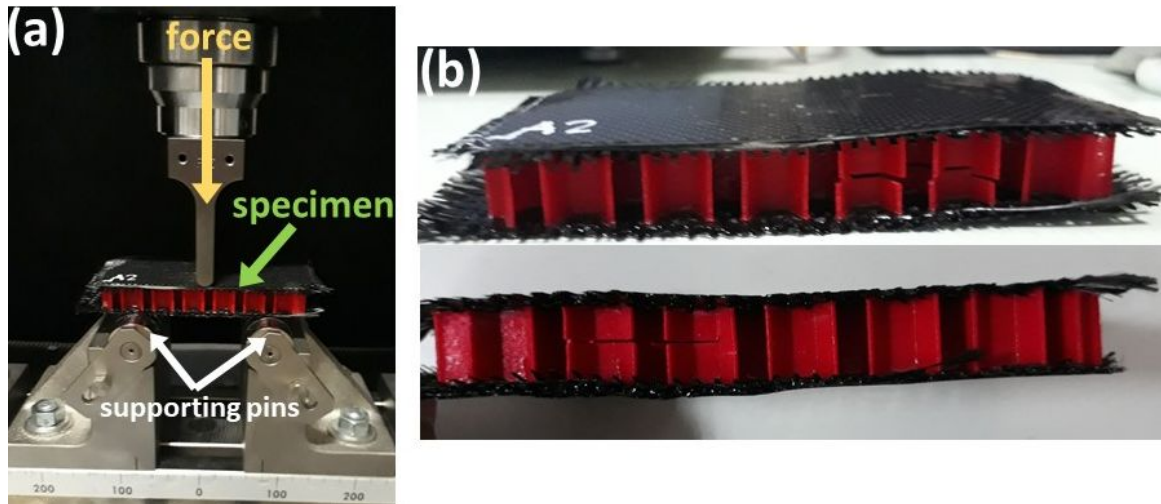


Figure 7. Image of a sandwich specimen; (a) in the flexural test, (b) after the flexural test

Table 3. Flexural test results of sandwich composites

Specimens	Maximum load (N)	Flexural strength (MPa)	Flexural stiffness (N/mm)
H-PLA	1242.081 ± 27.92	44.233 ± 0.99	638.516 ± 51.88
H-CFR-PLA	1627.286 ± 147.36	57.951 ± 5.25	1120.400 ± 111.44
S-PLA	2171.066 ± 192.29	77.317 ± 6.85	1419.400 ± 92.93
S-CFR-PLA	2372.672 ± 136.37	80.926 ± 4.86	1506.336 ± 101.95
D-PLA	4177.550 ± 250.67	144.618 ± 6.96	2472.244 ± 109.16
D-CFR-PLA	4846.821 ± 165.07	183.137 ± 3.84	3261.775 ± 94.39

Flexural load-deflection curves of sandwich composite specimens are given in Figure 8. Typically, the sandwich specimens exhibited a linear elastic region until they reached the point of maximum force. In all three core structures, composites containing carbon fiber-reinforced PLA filament showed higher flexural strength and flexural stiffness than those produced with pure PLA filament (Figures 9a and 9b). Among the composite specimens, H-PLA showed the lowest flexural strength and stiffness with values of 44.232 MPa and 638.516 N/mm, respectively. In the case of H-CFR-PLA, the flexural strength and flexural stiffness are 57.951 MPa and 1120.4 N/mm, respectively. S-CFR-PLA showed approximately 4.47% and 6.12% greater values of flexural strength and stiffness than S-PLA. D-CFR-PLA showed the highest flexural strength and stiffness with values of 183.137 MPa and 3261.775 N/mm, respectively. In a study by Liao et al., composite specimens were produced with PA12 filaments containing carbon fiber in different additive ratios (0, 2, 4, 6, 8, and 10%) by the FDM method and their mechanical properties were investigated. They stated that the flexural strength increased as the amount

of carbon fiber increased, and the composite containing 10% by weight carbon fiber-PA12 showed 251.1% higher flexural strength than the composite produced with pure PA12 filament [76]. Similar results were observed in articles [67, 77, 78].

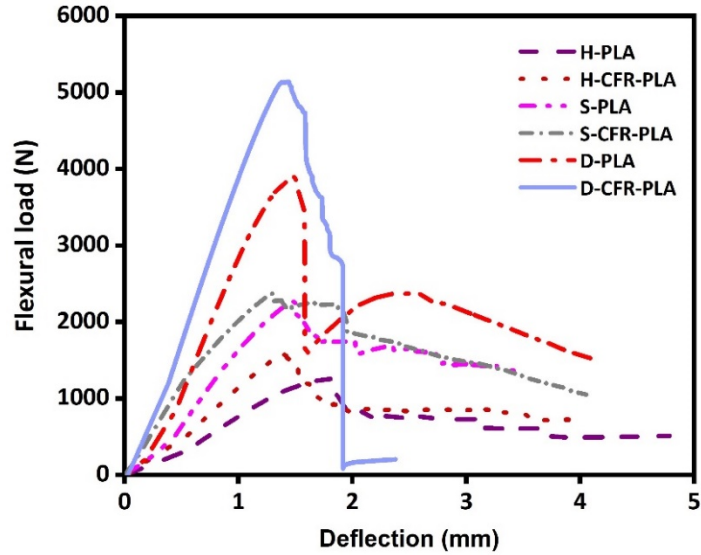


Figure 8. Flexural load- deflection curve of sandwich composite specimens

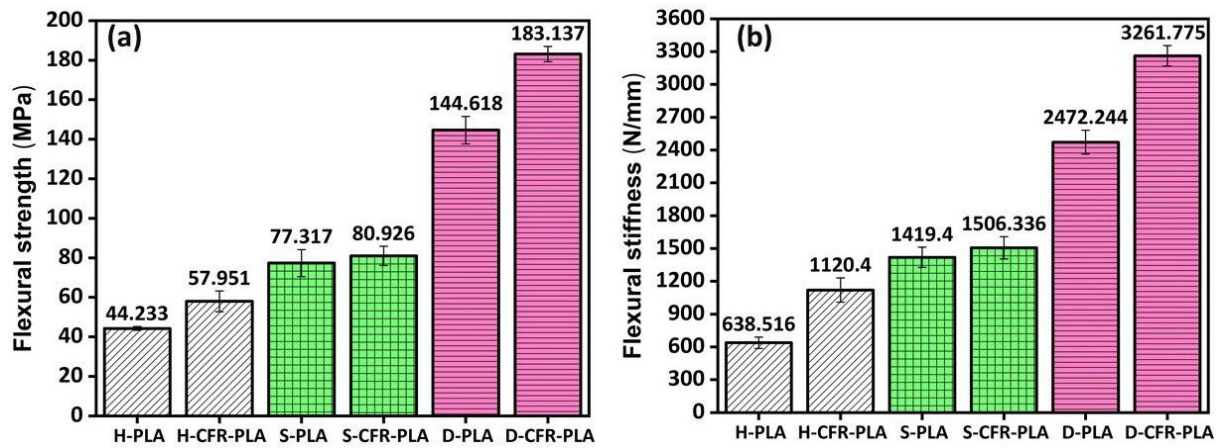


Figure 9. Flexural strength (a) and flexural stiffness (b) of sandwich composite specimens

#### IV. CONCLUSIONS

Stronger and lighter three-dimensional parts are produced by depositing the materials layer by layer using the additive manufacturing (AM) method. Among the AM methods, the most widely used one is the fused deposition modeling (FDM) method. In this study, it is aimed to produce different core structures that can be used in unmanned aerial vehicles (UAVs) by using the FDM method. For this purpose, a new structure was developed as an alternative to the honeycomb and square structures frequently encountered in the literature. Firstly, honeycomb,

square and designed structures were 3D printed with both PLA and carbon fiber-reinforced PLA filaments and then, sandwich composites were produced by adding carbon fiber fabric-epoxy to the lower and upper surfaces of these core structures. Experimental studies were carried out to investigate the effects of carbon fiber addition to PLA filaments on the mechanical properties of different lattice structures. The lattice structures containing carbon fiber reinforced-PLA filament showed lower compressive strength than those without reinforcement and the highest compressive strength was seen in the designed structure with a value of 9.867 MPa. D-PLA exhibited 32.18% and 54.36% higher tensile strength than H-PLA and S-PLA, respectively. In the flexural test results, it was observed that the flexural strength and stiffness values of the sandwich composites increased with the addition of 15 wt% carbon fiber reinforcement in the PLA filament. With the carbon fiber reinforcement, the flexural strengths of the sandwich composites containing honeycomb, square and designed lattice structures increased by approximately 31.01%, 4.67%, and 26.63%, respectively. In the subsequent studies, the aim is to produce various core structures using filled-filaments and investigate their mechanical properties. It will be recommended to use sandwich composites produced from these core structures in UAVs.

#### **ACKNOWLEDGMENT**

The authors would like to thank for the financial support of this research to the TUBITAK (Scientific and Technological Research Council of Turkey) 2209-B University Students Research Projects Support Program (project no: 1139B411901075). In addition, the authors thank the BAYKAR Inc. for supplying the carbon fabric. This article is based upon work from COST Action “High-performance Carbon-based composites with Smart properties for Advanced Sensing Applications” (EsSENce Cost Action CA19118, <http://www.essence-cost.eu/>) supported by COST (European Cooperation in Science and Technology, <https://www.cost.eu>).

#### **DECLARATION OF INTEREST STATEMENT**

The authors declare that they have no known competing financial interests or personal relationships that could have appeared to influence the work reported in this paper.

#### **FUNDING**

This study was supported under the TUBITAK (Scientific and Technological Research Council of Turkey) 2209-B University Students Research Projects Support Program (project no: 1139B411901075).

#### **REFERENCES**

- [1] Ukaegbu UF, Tartibu LK, Okwu MO, Olayode IO (2021) Development of a light-weight unmanned aerial vehicle for precision agriculture. *Sensors* 21:4417.
- [2] Vogeltanz T (2016) A survey of free software for the design, analysis, modelling, and simulation of an unmanned aerial vehicle. *Arch Comput Methods Eng* 23:449–514.
- [3] Goh GD, Agarwala S, Goh GL, Dikshit V, Sing SL, Yeong WY (2017) Additive manufacturing in unmanned aerial vehicles (UAVs): Challenges and potential. *Aerosp Sci Technol* 63:140–151.
- [4] Li J (2022) Artificial intelligence technology and China’s defense system. *J. Indo-Pacific Aff.* <https://www.airuniversity.af.edu/JIPA/Display/Article/2980879/artificialintelligence-technology-and-chinas-defense-system/#sdendnote1sym>. Accessed 15 June 2023.

- [5] Bi ZM, Yung KL, Ip AWH, Tang YK, Zhang CWJ, Xu L Da (2022) The state of the art of information integration in space applications. *IEEE Access* 10: 110110-110135.
- [6] Cawthorne D (2023) The ethics of drone design: how value-sensitive design can create better technologies. Taylor & Francis.
- [7] Shavarani SM, Nejad MG, Rismanchian F, Izbirak G (2018) Application of hierarchical facility location problem for optimization of a drone delivery system: a case study of Amazon prime air in the city of San Francisco. *Int J Adv Manuf Technol* 95:3141–3153.
- [8] Saari M, Cox B, Richer E, Krueger PS, Cohen AL (2015) Fiber encapsulation additive manufacturing: An enabling technology for 3D printing of electromechanical devices and robotic components. *3D Print Addit Manuf* 2:32–39.
- [9] Moon SK, Tan YE, Hwang J, Yoon Y-J (2014) Application of 3D printing technology for designing light-weight unmanned aerial vehicle wing structures. *Int J Precis Eng Manuf Technol* 1:223–228.
- [10] Klippstein H, Diaz De Cerio Sanchez A, Hassanin H, Zweiri Y, Seneviratne L (2018) Fused deposition modeling for unmanned aerial vehicles (UAVs): a review. *Adv Eng Mater* 20:1700552.
- [11] Emimi M, Khaleel M, Alkrash A (2023) The current opportunities and challenges in drone technology. *Int J Electr Eng Sustain* 1:74–89.
- [12] Borchardt JK (2004) Unmanned aerial vehicles spur composites use. *Reinf Plast* 48:28–31
- [13] Dikshit V, Yap YL, Goh GD, Yang H, Lim JC, Qi X, Yeong WY, Wei J (2016) Investigation of out of plane compressive strength of 3D printed sandwich composites. In: *IOP Conf. Ser. Mater. Sci. Eng.* IOP Publishing, p 12017.
- [14] Fu X, Lin Y, Yue X-J, XunMa, Hur B, Yue X-Z (2022) A review of additive manufacturing (3D printing) in aerospace: Technology, materials, applications, and challenges. In: *Mob. Wirel. Middleware, Oper. Syst. Appl. 10th Int. Conf. Mob. Wirel. Middleware, Oper. Syst. Appl. (MOBILWARE 2021)*. Springer, pp 73–98.
- [15] Goh GD, Toh W, Yap YL, Ng TY, Yeong WY (2021) Additively manufactured continuous carbon fiber-reinforced thermoplastic for topology optimized unmanned aerial vehicle structures. *Compos Part B Eng* 216:108840.
- [16] Praveena BA, Lokesh N, Buradi A, Santhosh N, Praveena BL, Vignesh R (2022) A comprehensive review of emerging additive manufacturing (3D printing technology): Methods, materials, applications, challenges, trends and future potential. *Mater Today Proc* 52:1309–1313.
- [17] Lee JM, Yeong WY (2016) Design and printing strategies in 3D bioprinting of cell-hydrogels: A review. *Adv Healthc Mater* 5:2856–2865.
- [18] Tom T, Sreenilayam SP, Brabazon D, Jose JP, Joseph B, Madanan K, Thomas S (2022) Additive manufacturing in the biomedical field-recent research developments. *Results Eng* 100661.
- [19] Srivastava M, Rathee S, Patel V, Kumar A, Koppad PG (2022) A review of various materials for additive manufacturing: Recent trends and processing issues. *J Mater Res Technol* 21:2612–2641.
- [20] Cramer CL, Ionescu E, Graczyk-Zajac M, Nelson AT, Katoh Y, Haslam JJ, Wondraczek L, Aguirre TG, LeBlanc S, Wang H (2022) Additive manufacturing of ceramic materials for energy applications: Road map and opportunities. *J Eur Ceram Soc* 42:3049–3088.
- [21] Ren L, Wang Z, Ren L, Han Z, Liu Q, Song Z (2022) Graded biological materials and additive manufacturing technologies for producing bioinspired graded materials: An overview. *Compos Part B Eng* 242:110086.
- [22] Chaudhary RP, Parameswaran C, Idrees M, Rasaki AS, Liu C, Chen Z, Colombo P (2022) Additive manufacturing of polymer-derived ceramics: Materials, technologies, properties and potential applications. *Prog Mater Sci* 128:100969.
- [23] Madhavadas V, Srivastava D, Chadha U, Raj SA, Sultan MTH, Shahar FS, Shah AUM (2022) A review on metal additive manufacturing for intricately shaped aerospace components. *CIRP J Manuf Sci Technol* 39:18–36.
- [24] Ramazani H, Kami A (2022) Metal FDM, a new extrusion-based additive manufacturing technology for manufacturing of metallic parts: a review. *Prog Addit Manuf* 7:609–626.
- [25] Megdich A, Habibi M, Laperriere L (2023) A review on 4D printing: Material structures, stimuli and additive manufacturing techniques. *Mater Lett* 133977.
- [26] Najmon JC, Raeisi S, Tovar A (2019) Review of additive manufacturing technologies and applications in the aerospace industry. *Addit Manuf Aerosp Ind* 7–31.
- [27] Easter S, Turman J, Sheffler D, Balazs M, Rotner J (2013) Using advanced manufacturing to produce unmanned aerial vehicles: a feasibility study. In: *Ground/air Multisens. interoperability, Integr. Netw. persistent ISR IV*. SPIE, pp 20–35.
- [28] Šančić T, Brčić M, Kotarski D, Łukaszewicz A (2023) Experimental characterization of composite-printed materials for the production of multicopter UAV airframe parts. *Materials (Basel)* 16:5060.
- [29] Azarov A V, Antonov FK, Golubev M V, Khaziev AR, Ushanov SA (2019) Composite 3D printing for the small size unmanned aerial vehicle structure. *Compos Part B Eng* 169:157–163.

- [30] Grodzki W, Łukaszewicz A (2015) Design and manufacture of unmanned aerial vehicles (uav) wing structure using composite materials: Planung und bau einer flügelstruktur für unbemannte luftfahrzeuge (uav) unter verwendung von kompositwerkstoffen. *Materwiss Werksttech* 46:269–278.
- [31] Dudek P (2013) FDM 3D printing technology in manufacturing composite elements. *Arch Metall Mater* 58:1415–1418.
- [32] Stern M, Cohen E (2013) VAST AUAV (variable airspeed telescoping additive unmanned air vehicle). In *Technical Paper - Society of Manufacturing Engineers*, TP13PUB47.
- [33] Sugiyama K, Matsuzaki R, Ueda M, Todoroki A, Hirano Y (2018) 3D printing of composite sandwich structures using continuous carbon fiber and fiber tension. *Compos Part A Appl Sci Manuf* 113:114–121.
- [34] Goh GD, Yap YL, Agarwala S, Yeong WY (2019) Recent progress in additive manufacturing of fiber reinforced polymer composite. *Adv Mater Technol* 4:1800271.
- [35] Jayanth N, Senthil P, Prakash C (2018) Effect of chemical treatment on tensile strength and surface roughness of 3D-printed ABS using the FDM process. *Virtual Phys Prototyp* 13:155–163.
- [36] Szykiedans K, Credo W (2016) Mechanical properties of FDM and SLA low-cost 3-D prints. *Procedia Eng* 136:257–262.
- [37] Ning F, Cong W, Qiu J, Wei J, Wang S (2015) Additive manufacturing of carbon fiber reinforced thermoplastic composites using fused deposition modeling. *Compos Part B Eng* 80:369–378.
- [38] Zhong W, Li F, Zhang Z, Song L, Li Z (2001) Short fiber reinforced composites for fused deposition modeling. *Mater Sci Eng A* 301:125–130.
- [39] Namiki M, Ueda M, Todoroki A, Hirano Y, Matsuzaki R (2014) 3D printing of continuous fiber reinforced plastic. *SAMPE Tech Seattle 2014 Conf, Seattle, United States, June 2-5*.
- [40] Shofner ML, Lozano K, Rodríguez-Macías FJ, Barrera E V (2003) Nanofiber-reinforced polymers prepared by fused deposition modeling. *J Appl Polym Sci* 89:3081–3090.
- [41] Khan ZI, Mohamad Z, Rahmat AR, Habib U (2021) Synthesis and characterization of composite materials with enhanced thermo-mechanical properties for unmanned aerial vehicles (uavs) and aerospace technologies. *Pertanika J. Sci. Technol* 29:2003-2015.
- [42] Ning F, Cong W, Hu Y, Wang H (2017) Additive manufacturing of carbon fiber-reinforced plastic composites using fused deposition modeling: Effects of process parameters on tensile properties. *J Compos Mater* 51:451–462.
- [43] Zhang W, Cotton C, Sun J, Heider D, Gu B, Sun B, Chou T-W (2018) Interfacial bonding strength of short carbon fiber/acrylonitrile-butadiene-styrene composites fabricated by fused deposition modeling. *Compos Part B Eng* 137:51–59.
- [44] Ferreira RTL, Amatte IC, Dutra TA, Bürger D (2017) Experimental characterization and micrography of 3D printed PLA and PLA reinforced with short carbon fibers. *Compos Part B Eng* 124:88–100.
- [45] Zhang H, Zhang L, Zhang H, Wu J, An X, Yang D (2021) Fibre bridging and nozzle clogging in 3D printing of discontinuous carbon fibre-reinforced polymer composites: Coupled CFD-DEM modelling. *Int J Adv Manuf Technol* 117:3549–3562.
- [46] Van de Werken N, Tekinalp H, Khanbolouki P, Ozcan S, Williams A, Tehrani M (2020) Additively manufactured carbon fiber-reinforced composites: State of the art and perspective. *Addit Manuf* 31:100962.
- [47] Quan Z, Larimore Z, Wu A, Yu J, Qin X, Mirotznik M, Suhr J, Byun J-H, Oh Y, Chou T-W (2016) Microstructural design and additive manufacturing and characterization of 3D orthogonal short carbon fiber/acrylonitrile-butadiene-styrene preform and composite. *Compos Sci Technol* 126:139–148.
- [48] Lupone F, Padovano E, Venezia C, Badini C (2022) Experimental characterization and modeling of 3D printed continuous carbon fibers composites with different fiber orientation produced by FFF process. *Polymers* 14:426.
- [49] Justo J, Távara L, García-Guzmán L, París F (2018) Characterization of 3D printed long fibre reinforced composites. *Compos Struct* 185:537–548.
- [50] Iragi M, Pascual-González C, Esnaola A, Lopes CS, Aretxabaleta L (2019) Ply and interlaminar behaviours of 3D printed continuous carbon fibre-reinforced thermoplastic laminates; effects of processing conditions and microstructure. *Addit Manuf* 30:100884.
- [51] Chacón JM, Caminero MA, Núñez PJ, García-Plaza E, García-Moreno I, Reverte JM (2019) Additive manufacturing of continuous fibre reinforced thermoplastic composites using fused deposition modelling: Effect of process parameters on mechanical properties. *Compos Sci Technol* 181:107688.
- [52] Borowski A, Vogel C, Behnisch T, Geske V, Gude M, Modler N (2021) Additive manufacturing-based in situ consolidation of continuous carbon fibre-reinforced polycarbonate. *Materials* 14:2450.
- [53] Xiao L, Xu X, Feng G, Li S, Song W, Jiang Z (2022) Compressive performance and energy absorption of additively manufactured metallic hybrid lattice structures. *Int J Mech Sci* 219:107093.
- [54] Sarvestani HY, Akbarzadeh AH, Niknam H, Hermenean K (2018) 3D printed architected polymeric sandwich panels: Energy absorption and structural performance. *Compos Struct* 200:886–909.

- [55] Al-Ketan O, Lee D-W, Al-Rub RKA (2021) Mechanical properties of additively-manufactured sheet-based gyroidal stochastic cellular materials. *Addit Manuf* 48:102418.
- [56] Herrmann C, Dewulf W, Hauschild M, Kaluza A, Kara S, Skerlos S (2018) Life cycle engineering of lightweight structures. *CIRP Ann* 67:651–672.
- [57] Galos J, Das R, Sutcliffe MP, Mouritz AP (2022) Review of balsa core sandwich composite structures. *Mater Des* 221:111013.
- [58] Cao D, Bouzolin D, Lu H, Griffith DT (2023) Bending and shear improvements in 3D-printed core sandwich composites through modification of resin uptake in the skin/core interphase region. *Compos Part B Eng* 264:110912.
- [59] Zaharia SM, Pop MA, Chicos L-A, Buican GR, Lancea C, Pascariu IS, Stamate V-M (2022) Compression and bending properties of short carbon fiber reinforced polymers sandwich structures produced via fused filament fabrication process. *Polymers* 14:2923.
- [60] Sarvestani HY, Akbarzadeh AH, Mirbolghasemi A, Hermenean K (2018) 3D printed meta-sandwich structures: Failure mechanism, energy absorption and multi-hit capability. *Mater Des* 160:179–193.
- [61] Ingrole A, Hao A, Liang R (2017) Design and modeling of auxetic and hybrid honeycomb structures for in-plane property enhancement. *Mater Des* 117:72–83.
- [62] Gautam R, Idapalapati S, Feih S (2018) Printing and characterisation of Kagome lattice structures by fused deposition modelling. *Mater Des* 137:266–275.
- [63] Schaedler TA, Carter WB (2016) Architected cellular materials. *Annu Rev Mater Res* 46:187–210.
- [64] Lu C, Qi M, Islam S, Chen P, Gao S, Xu Y, Yang X (2018) Mechanical performance of 3D-printing plastic honeycomb sandwich structure. *Int J Precis Eng Manuf Technol* 5:47–54.
- [65] Tao Y, Li W, Wei K, Duan S, Wen W, Chen L, Pei Y, Fang D (2019) Mechanical properties and energy absorption of 3D printed square hierarchical honeycombs under in-plane axial compression. *Compos Part B Eng* 176:107219.
- [66] C365-03: Standard Test Method for Flatwise Compressive Properties of Sandwich Cores (2003). ASTM International, West Conshohocken.
- [67] Abeykoon C, Sri-Amphorn P, Fernando A (2020) Optimization of fused deposition modeling parameters for improved PLA and ABS 3D printed structures. *Int J Light Mater Manuf* 3:284–297.
- [68] Shanmugam V, Rajendran DJJ, Babu K, Rajendran S, Veerasimman A, Marimuthu U, Singh S, Das O, Neisiany RE, Hedenqvist MS (2021) The mechanical testing and performance analysis of polymer-fibre composites prepared through the additive manufacturing. *Polym Test* 93:106925.
- [69] Sood AK, Ohdar RK, Mahapatra SS (2012) Experimental investigation and empirical modelling of FDM process for compressive strength improvement. *J Adv Res* 3:81–90.
- [70] Mieszala M, Hasegawa M, Guillonneau G, Bauer J, Raghavan R, Frantz C, Kraft O, Mischler S, Michler J, Philippe L (2017) Micromechanics of amorphous metal/polymer hybrid structures with 3D cellular architectures: size effects, buckling behavior, and energy absorption capability. *Small* 13:1602514.
- [71] Babamiri BB, Askari H, Hazeli K (2020) Deformation mechanisms and post-yielding behavior of additively manufactured lattice structures. *Mater Des* 188:108443.
- [72] Mei H, Yin X, Zhang J, Zhao W (2019) Compressive properties of 3D printed polylactic acid matrix composites reinforced by short fibers and SiC nanowires. *Adv Eng Mater* 21:1800539.
- [73] Saleh M, Anwar S, Al-Ahmari AM, Alfaiy A (2022) Compression performance and failure analysis of 3D-printed carbon fiber/PLA composite TPMS lattice structures. *Polymers (Basel)* 14:4595.
- [74] Van Der Klift F, Koga Y, Todoroki A, Ueda M, Hirano Y, Matsuzaki R (2016) 3D printing of continuous carbon fibre reinforced thermo-plastic (CFRTP) tensile test specimens. *Open J Compos Mater* 6:18-27.
- [75] Mohan N, Senthil P, Vinodh S, Jayanth N (2017) A review on composite materials and process parameters optimisation for the fused deposition modelling process. *Virtual Phys Prototyp* 12:47–59.
- [76] Liao G, Li Z, Cheng Y, Xu D, Zhu D, Jiang S, Guo J, Chen X, Xu G, Zhu Y (2018) Properties of oriented carbon fiber/polyamide 12 composite parts fabricated by fused deposition modeling. *Mater Des* 139:283–292.
- [77] Gavali VC, Kubade PR, Kulkarni HB (2020) Property enhancement of carbon fiber reinforced polymer composites prepared by fused deposition modeling. *Mater Today Proc* 23:221–229.
- [78] Sang L, Han S, Li Z, Yang X, Hou W (2019) Development of short basalt fiber reinforced polylactide composites and their feasible evaluation for 3D printing applications. *Compos Part B Eng* 164:629–639.